Analysis of Oxygen Inhibition in Photopolymerizations of Hydrogel Micropatterns Using FTIR Imaging

Dipti Biswal and J. Z. Hilt*

Chemical and Materials Engineering, University of Kentucky, Lexington, Kentucky 40506

Received July 16, 2008; Revised Manuscript Received December 9, 2008

ABSTRACT: UV photopolymerizations are a versatile polymerization technique and are thus utilized in a variety of applications. Photopolymerizations are often free-radical polymerizations, and these reactions (e.g., final conversion and reaction rates) can be inhibited by the presence of oxygen. In particular, oxygen inhibition can play a critical role in polymerization process occurring in thin films and micro/nanoscale structures where oxygen is able to rapidly transport through the short diffusion paths. Since patterned polymer micro- and nanostructures are of high interest in a variety of applications (e.g., biomedical microdevices), there is a need for methods to characterize polymerization processes at the small scale. Here, a novel method was applied to fabricate thin film of hydrogel microstructure on gold surface by using microcontact printing. The photopolymerization reaction of the patterned hydrogel was studied in situ and spatially resolved in real time with FTIR imaging techniques. The effect of oxygen inhibition during photopolymerization was also analyzed using FTIR imaging. The oxygen inhibition during polymerization was reduced by increasing the amount of photoinitiator or increasing UV intensity. This novel fabrication and characterization method will facilitate the optimization of integration processes of patterned hydrogel films.

Introduction

The inability of free radical photopolymerizations to overcome oxygen inhibition has limited their applicability and in many cases forced the application of inerting equipment. The synthesis and characterization of patterned hydrogel structures at the micro- and nanoscale is critical for many applications, but currently, limited methods are available for the synthesis and characterization of hydrogels at the micro- and nanoscale. In particular, no methods are available to synthesize the micropatterned hydrogel and simultaneously study the effect of oxygen inhibition during the polymerization. Here, we have demonstrated a novel method for patterning thin hydrogel films on gold surface via photopolymerizations and studied the effect of oxygen inhibition of those thin patterned polymer film via FTIR imaging system.

Hydrogels are hydrophilic polymer networks that swell to a high degree in water or biological fluids due to an extremely high affinity for water yet are insoluble because of the incorporation of chemical or physical cross-links. Because of this high water content and the corresponding rubbery nature, hydrogels are similar to a variety of natural living tissues. This has led to widespread application of hydrogels as biomaterials, such as in contact lenses, sutures, dental materials, and controlled drug delivery devices.[1−4] By tailoring the various functional groups along the polymer backbone, hydrogels can be designed to have responsive swelling properties when subjected to changes in the surrounding ambient conditions. The unique ability of reversible swelling and shrinking makes them attractive for various actuation applications. A small change in the surrounding environment can result in an increase or decrease in volume, but these responses can be very slow for bulk systems. Micro- and nanoscale hydrogel structures have a faster response to a stimulus due to their short length scales and high surface-to-volume ratio. Because of their stimuli response nature, patterned hydrogel structures have potential application in microfluidics,[5] tissue engineering,[6] biological and chemical sensors,[7,8] and other soft matter technologies.

The ability to pattern hydrogel structures at the small scale is very important for many applications in cell biology, tissue engineering, microdevices, etc. Environmentally responsive hydrogels have been used as functional components of microdevices, including biosensors and valves. For example, micropatterned hydrogels have been used within a microchannel as a valve that can sense a pH change and actuate for use in microdevice applications.[5,9] Also, environmentally responsive hydrogels have been patterned on silicon microcantilevers to develop an ultrasensitive microsensor.[10,11] Additionally, there has been several groups developing and applying responsive hydrogels as microvalves and micropumps.[12−14] Though various fabrication techniques available for the synthesis of these hydrogels, the methods for fabricating precise 3-D patterns of hydrogel at micro- and nanoscale on surfaces are limited.

Conventional FTIR microscopy has been around for many years and proven to be a valuable research tool, yet it has limitations due to its spatial resolution and long acquisition times.[15] Since first being developed a decade ago,[16] FTIR microscopes utilizing a focal plane array (FPA) detector have become the start-of-the-art in FTIR imaging.[17] In the past several years, FTIR imaging has been utilized in a wide variety of applications, where it is advantageous to acquire chemical information with microscale resolution. It has been used for the histopathological recognition[18] and the characterization of tissue-engineered bone and cartilage.[19] Several other researchers have utilized FTIR imaging to examine drug release processes,[20−22] polymer dissolution,[23,24] pharmaceutical formulation,[25] and photodegradation of polymer thin films.[26] However, there have not been any in-situ studies of photopolymerization kinetics of micropatterning reactions by FTIR imaging.

The influence of oxygen in a free radical photopolymerization has attracted significant interest for several years, since free radical polymerizations are inhibited by oxygen. It is desirable to carry out photopolymerizations in air, and therefore, methods for preventing oxygen inhibition processes are of high interest. Oxygen inhibition effects free radical polymerizations by slowing polymerization rates, increasing induction periods, decreasing conversion, decreasing polymer kinetic chain length,

* Corresponding author.

10.1021/ma801600c CCC: $40.75
Published on Web 01/27/2009

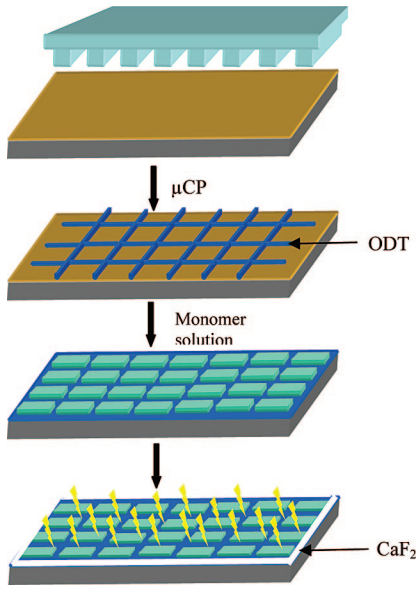

Figure 1. Schematic diagram of thiol monolayer formation and reaction setup.

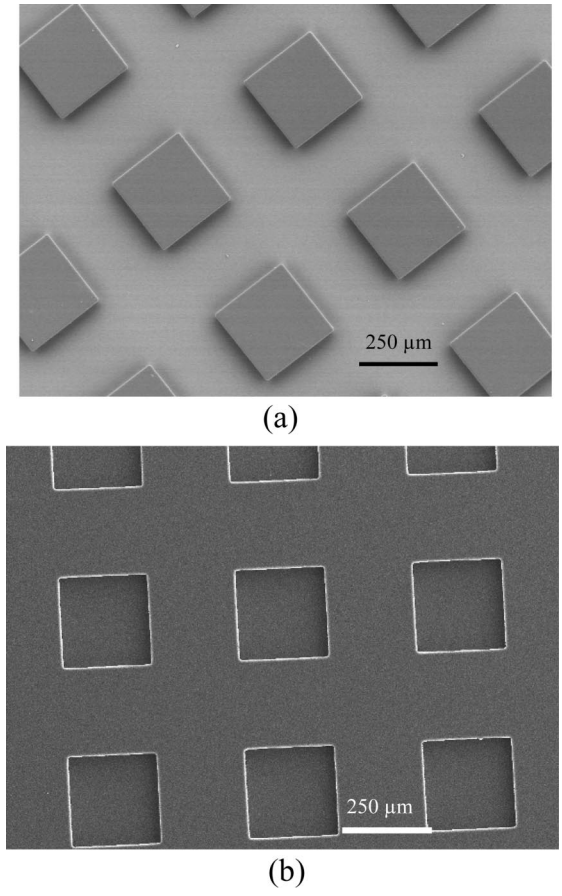

Figure 2. SEM images of the fabricated master chips (a) and PDMS stamp (b).

and creating tacky surface properties. Successful reduction in the sensitivity of photocuring systems to oxygen would provide a significant advantage in curing of thin films or coatings and also in micro- or nanoscale patterns. In very thin films and small patterns, oxygen continually diffuses across the small length scales of the reaction zone, scavenging all of the radicals and thus inhibiting the polymerization. The variance in conversion across a pattern or through a thin film will result in inhomogeneous materials and likely undesired physical or chemical properties. Several methods have been used to reduce the oxygen inhibition during the polymerization. Decker et al. used a dual initiator method in order to consume the dissolved oxygen in a monomer system prior to and during the polymerization.[27] The effect of oxygen inhibition can be also reduced by using different monomer systems.[28,29] Dickey et al. developed a quasi-steady-state approximation kinetic model to study the effect of oxygen diffusion at the etch barrier in step and flash Imprint lithography.[30] Recently, a comprehensive model including heat and mass transfer effects was applied to study the inhibitory effect of oxygen on free radical polymerization.[31] There have been limited or no methods applied to analyze the oxygen inhibition at microscale.

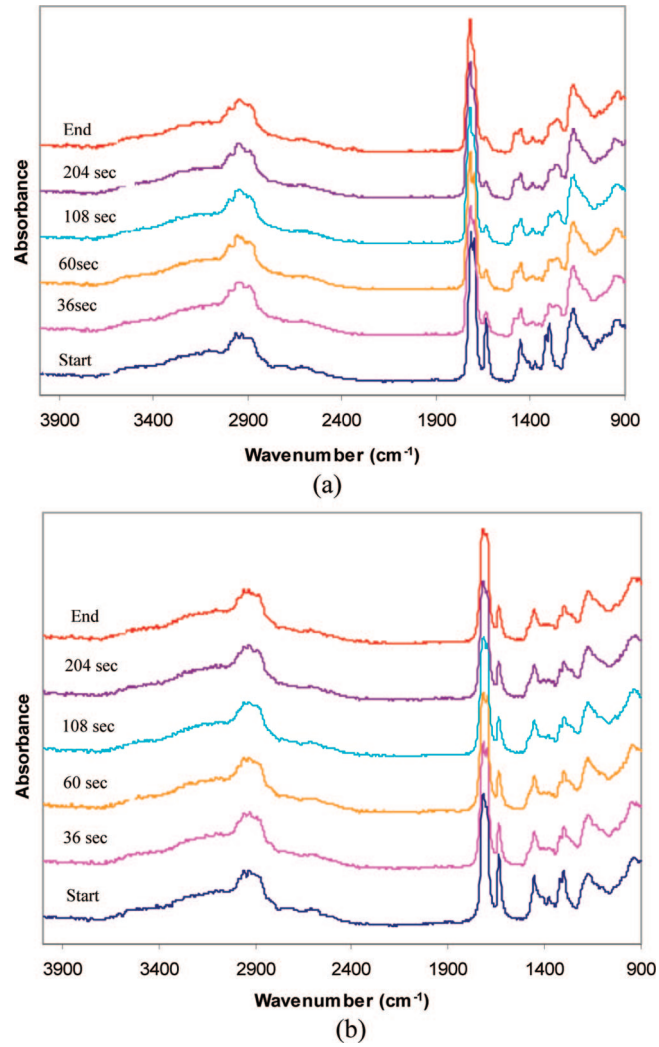

Figure 3. FTIR spectra collected from two different points A (a) and B (b) at different reaction times during the polymerization of hydrogel I.

Microcontact printing (μCP) is a simple technique for producing well-defined self-assembled monolayer patterns on different surfaces.[32,33] This technique is applicable to several types of inks and substrate, such as chemisorbing molecules onto metal or oxide surface,[34] reactants printed onto organic layers,[35] and protein transferred to silicon or glass surfaces.[36] For example, a reaction between the gold surface and a thiol molecule supplied by the stamp can result in the covalent assembly of a monolayer of the thiols on the gold substrate.

By using the method of polymerization controlled by microcontact printing (PCμCP),[37] it is possible to synthesize patterns over the gold surfaces. In this study, we have

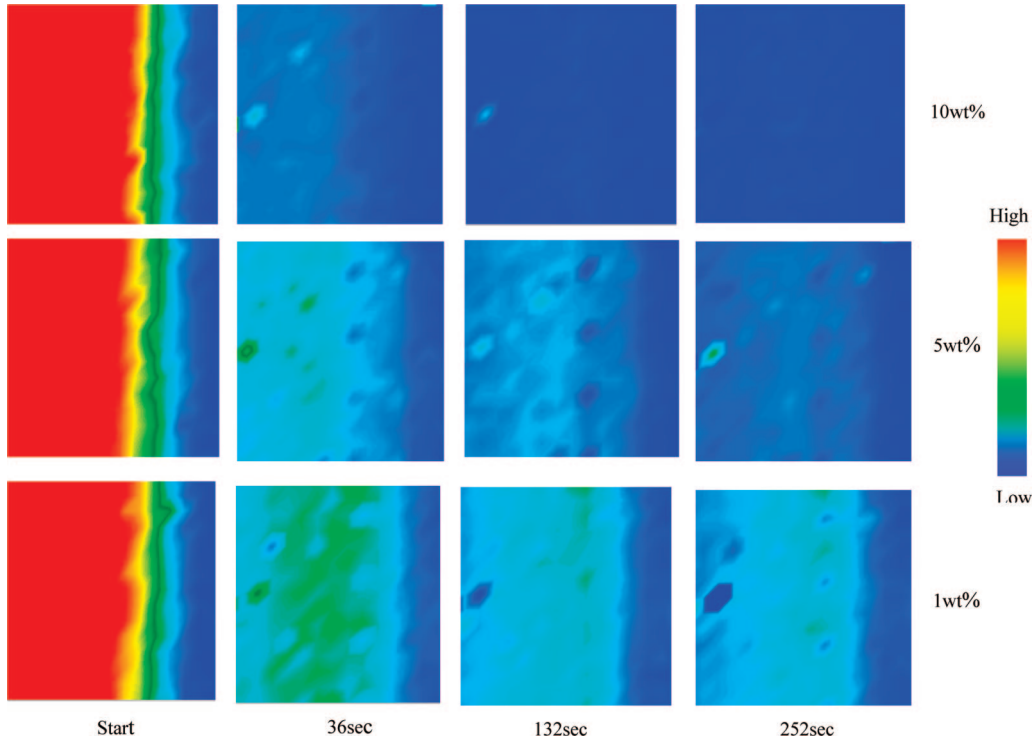

Figure 4. FTIR images of spectral slices extracted from 1634 cm^{-1} as a function of reaction time from patterned hydrogels I, II, and III. Scale bars indicate highest and lowest intensities, respectively.

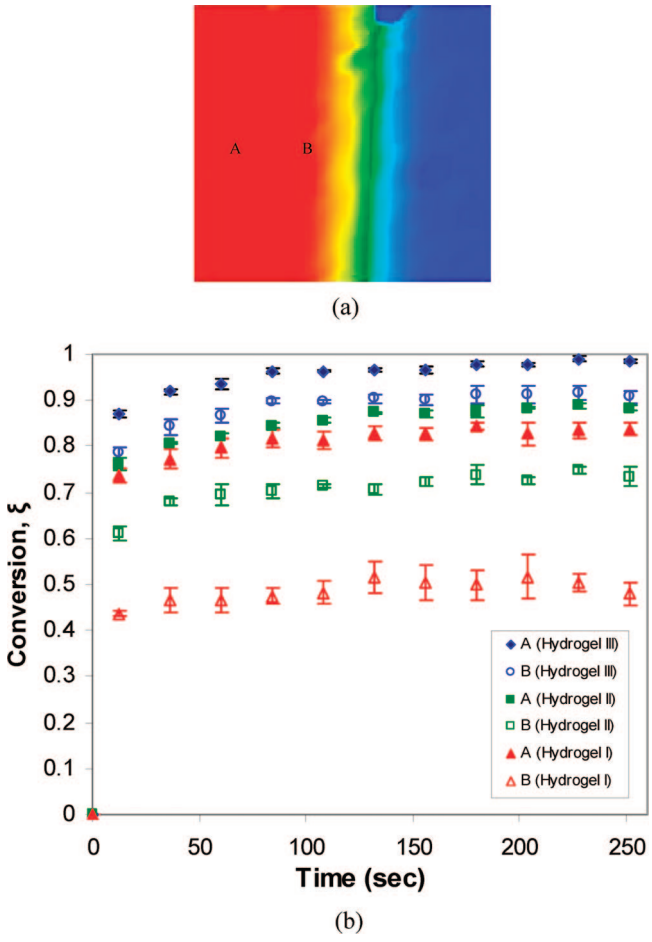

Figure 5. FTIR image of the focused patterned hydrogel showing point A and B (a). Conversion vs time curves of hydrogels I, II, and III at A and B (b).

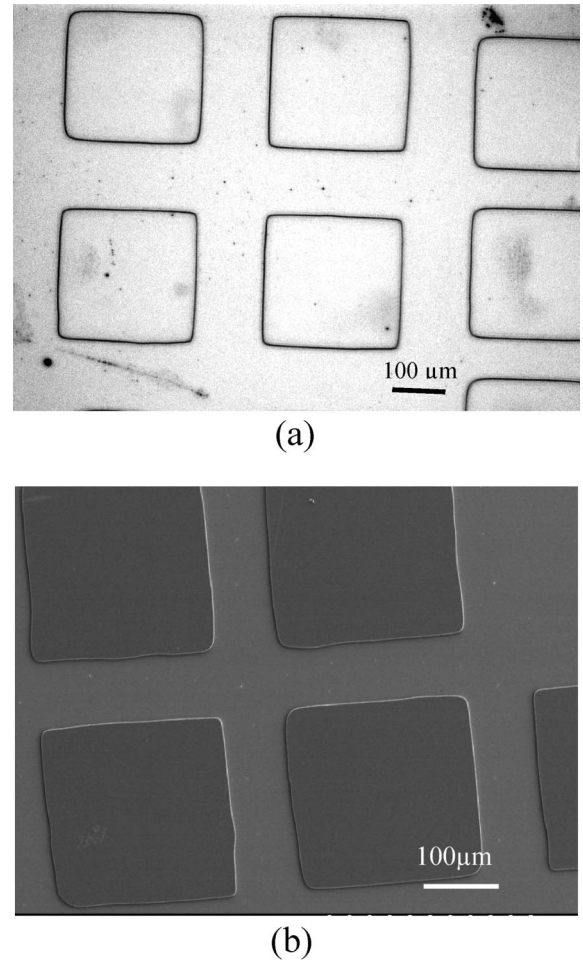

Figure 6. Optical (a) and SEM (b) images of the patterned hydrogel microstructures (hydrogel I).

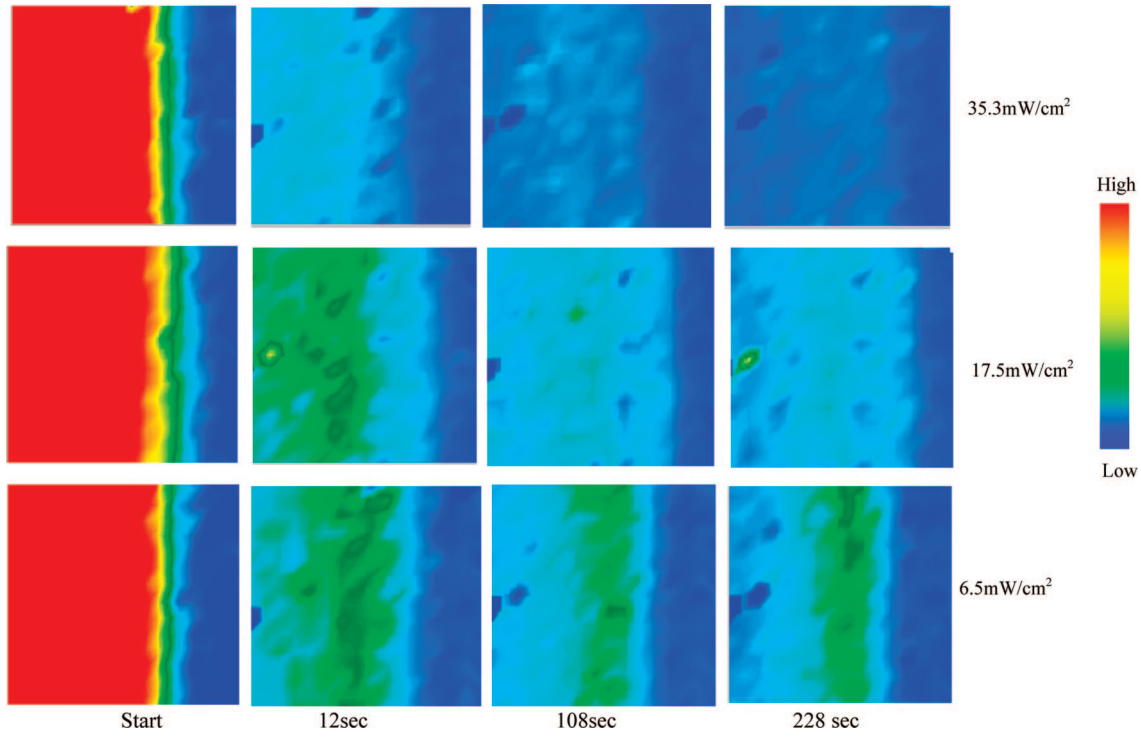

Figure 7. FTIR images of spectral slices extracted from 1634 cm^{-1} as a function of reaction time from patterned hydrogels IV, V, and VI. Scale bars indicate highest and lowest intensities, respectively.

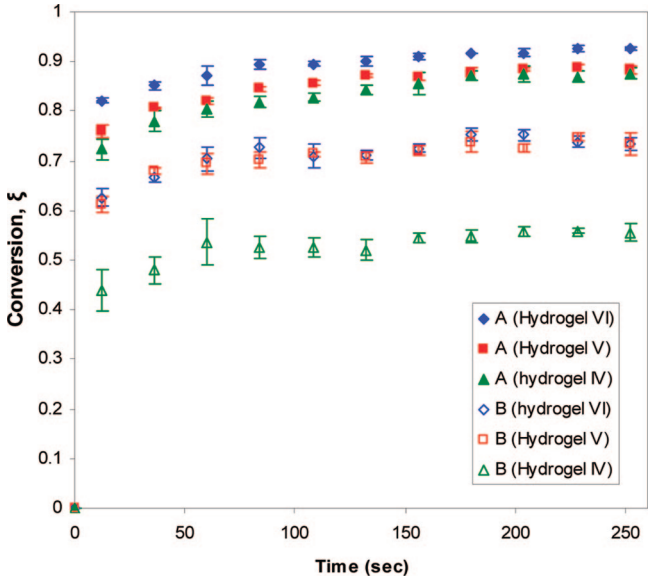

Figure 8. Conversion and time curves showing higher conversion at point A than point B for hydrogels IV, V, and VI.

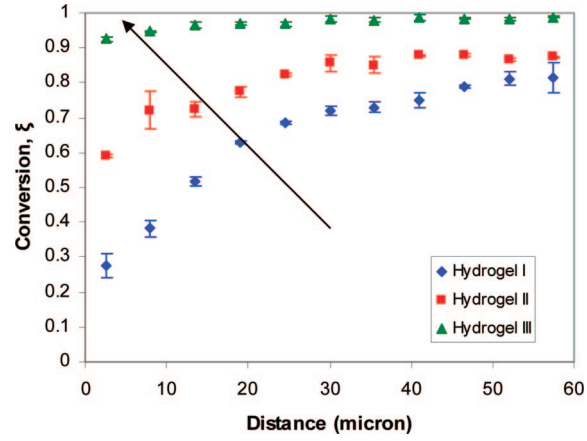

Figure 9. Conversion of patterned hydrogels I, II, and III across the surface with change in initiator concentration.

demonstrated a novel method using PCμCP to prepare controlled microscale reaction regions for patterning thin hydrogel films on gold surface and studying the effect of oxygen inhibition via FTIR imaging system during photopolymerization.

Experimental Section

Materials. The monomer system used for the experiment was a mixture of methacrylic acid (MAA) and cross-linker tetra(ethylene glycol) dimethacrylate (TEGDMA). The MAA was used after vacuum distillation, while all other chemicals were used as received. The monomer MAA and cross-linker TEGDMA were purchased from Polyscience, Inc. The UV photoinitiator, 2,2-dimethoxy-2-phenylacetophenone (DMPA), was purchased from Aldrich. The silicon and gold wafer used in this process were obtained from Virginia Semiconductor Inc. and Platypus Technologies, respectively. The gold substrate was an electron beam deposited gold film over a titanium layer on silicon. SU-8, an epoxy-based negative photoresist used for photolithography, was purchased from MicroChem Corp. (Newton, MA). Sylgard 184, a precursor solution for polydimethylsiloxane (PDMS), was donated by Dow Corning (Midland, MI). 1-Octadecanethiol (ODT) was purchased from Gelest.

Preparation of Master Chips and PDMS Stamp. The patterned master chips of different square sizes and thickness used for microcontact printing (μCP) were prepared by UV photolithography. The PDMS stamps replicated from master chips were prepared by using a 10:1 ratio of PDMS base and curing agent. The detailed procedure for the fabrication of master chips and PDMS stamp preparation is described elsewhere.[38]

Microcontact Printing and SAM Formation. Self-assembled monolayers of alkanethiol were patterned by μCP on the gold surface. The PDMS stamp was first inked by 1 mM solution of ODT in ethanol and blown dry in air for 10 s. Then, the PDMS

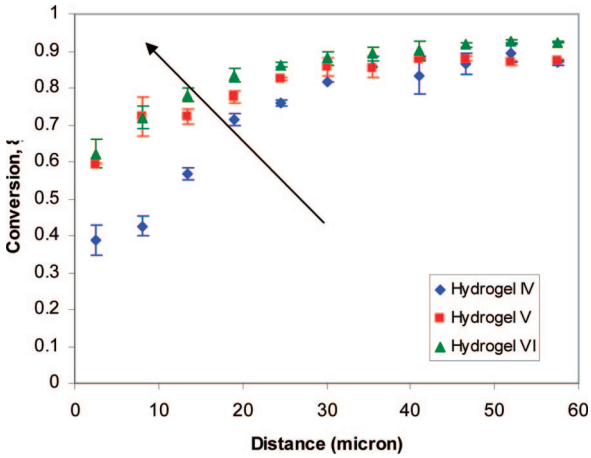

Figure 10. Conversion of patterned hydrogels IV, V, and VI across the surface with change in UV intensity.

stamp was brought in contact with freshly cleaned gold wafer for 30 s with slightly pressure to promote conformal contact between the stamp and substrate. Finally, the gold surface modified with SAMs was rinsed with ethanol and water and then dried. As a result of the features of the PDMS stamp, the SAMs remained between the squares, while the squares remained unmodified.

Micropatterned Hydrogel Formation. The photoinitiated polymerization reaction between MAA and TEGDMA was carried out using DMPA as photoinitiator. For hydrogel formation (hydrogel I), a monomer solution of 80:20 mol % of MAA and TEGDMA with 1 wt % of DMPA (total weight of monomer) was prepared, and then the solutions were applied to the patterned gold wafer. The monomer solutions remained only on the unmodified square zones. These hydrophobic and hydrophilic interactions successfully created the micropatterned regions containing hydrophilic monomer solution and hydrophobic thiol. In order to limit the oxygen inhibition to the planar interface during polymerization, the monomer solutions were covered by a CaF_2 window. This window assisted in the formation of a thin film of monomer solution. In order to study the reaction kinetics of the patterned hydrogel formation, the reaction assembly was placed under the FTIR microscope stage. A UV spot source (Omini cure series) was used to produce a UV intensity of 17.5 mW/cm^2. The UV spot light source employed had a wavelength ranging from $\lambda = 320-500$ nm. The polymerization reaction was carried out for 5 min. A schematic diagram of the above procedure is included in Figure 1. In order to study the effect of oxygen during polymerization, patterned hydrogel systems with the same monomer to cross-linker ratio but with different amounts of photoinitiator were also synthesized by using the above procedure. Patterned hydrogels with 5 and 10 wt % of initiator (hydrogels II and III) were prepared, and the reaction of each system was studied with the FTIR imaging system. For these studies, the UV intensity was kept fixed (17.5 mW/cm^2) for the synthesis (i.e., hydrogels I, II, and III). The effect of oxygen inhibition during the polymerization was also studied by varying the UV light intensity. For these patterned hydrogel microstructures (i.e., hydrogels IV, V, and VI) formation, 80:20 mol % of MAA and TEGDMA and 5 wt % of DMPA were used. The polymerization reactions were carried out at UV intensities of 6.5, 17.5, and 35.3 mW/cm^2 for hydrogels IV, V, and VI, respectively. Here, hydrogels II and V are identical systems.

Micropatterned Hydrogel Characterization. A Digilab Stingray system consisting of FTIR 7000e step scan spectrometer (Varian Inc.) and UMA 600 IR microscope was used to collect all the spectra and FTIR images. All spectra were collected in the range of 4000−900 cm^{-1} with a spectral resolution of 4 cm^{-1}, and 16 scans coaddition were used. A profilometer was used to measure the thickness of all the patterned hydrogels. Three separate measurements were conducted at different position of each sample to get the average thickness of the hydrogel microstructure. A scanning electron microscope (SEM, Hitachi S4300) was used to characterize the master chips, PDMS stamp, and the patterned hydrogels.

Results and Discussion

By using a photolithographic method, patterned master chips of different square sizes and thickness were fabricated successfully. PDMS stamps with the reverse features of these master chips were also prepared successfully. Figure 2 shows the SEM images of the master chips and PDMS stamp. The thicknesses of the patterned SAMs of thiol ODT were characterized by AFM, and the average thickness was 1.5 nm.[37]

The photoinitiated free radical polymerization was carried out successfully, with confirmation from the disappearance of the C═C peak. Figure 3 shows the FTIR spectra of hydrogel I at different reaction times at two different points in the patterned structures. Here, point A is toward the center of the square, and point B is near the edge of the patterned square (i.e., monomer/air interface). It is observed from these spectra that, as the reaction proceeded, the intensity of C═C peak at 1634 cm^{-1} decreased and eventually disappeared. However, there is clearly some unreacted monomer left at point B at the end of the reaction time, which is illustrated by the presence of peak at 1634 cm^{-1} (Figure 3b). Because of intermolecular or intramolecular hydrogen bonding between the carboxylic groups or between the carboxylic group and the oxygen group of TEGDMA, a broad peak at around 3430 cm^{-1} is observed with increasing reaction times.

Oxygen inhibits free radical polymerization by scavenging free radicals, and thus it disrupts the curing process. During the synthesis of the patterned hydrogels, the monomer solution was covered by a CaF_2 window. Thus, oxygen is only capable of diffusing from the planar interface where the monomer/air interface exists (i.e., from the sides of the square structures). In order to study the effect of oxygen inhibition during the photoinitiated polymerization of a patterned region, hydrogels with higher wt % of DMPA (hydrogels II and III) were synthesized. To visualize the patterning reaction of different systems via FTIR imaging, the edges of the square pattern were focused, facilitating the simultaneous analysis of reacting and nonreacting zones. For the comparison of the conversions of each system, the edges of the squares were fixed with a particular column of the FPA. For each system, scans at regular time intervals were carried out for the same focused position.

FTIR images were collected at every scan during the reaction time and plotted as a color gradient with the area of the 1634 cm^{-1} peak. Figure 4 shows the FTIR images of hydrogels I, II, and III at different time intervals. In each system, the reduction of C═C absorbance at 1634 cm^{-1} is clearly visualized with reaction time by changing the color gradient from red to blue. It has been clearly observed from Figure 4 that at 36 s there is a greater concentration of unreacted monomer near the edge of the square in hydrogel I in comparison to hydrogels II and III. However, at the end of the reaction, hydrogel III has a lower concentration of unreacted monomer near the interface. These FTIR images at particular time intervals give a clear illustration of the oxygen diffusion from the sides of the squares during the polymerization. Because of continuous oxygen diffusion from the sides of the squares, the monomer solution present near the edges of the square polymerizes slowly. The diffusion of oxygen to the center of the square is minimal, and thus, the monomer polymerizes faster at the center of the square in comparison to the edges.

To demonstrate the oxygen inhibition during polymerization, we analyze points A (toward the center) and B (near the edge) inside the square, which correspond to different pixels in a row of the FPA, at a particular reaction time (Figure 5a). The rate of conversion of double bonds of each spectrum at the points A and B was determined by standard baseline techniques using the peak area of the 1636 cm^{-1} for C═C vibration and the area of 1713 cm^{-1} for C═O stretching as reference.[38] From the conversion vs time curves, it has been clearly observed that for all the systems at a particular time the rate of conversion at point A was greater than B (Figure 5b). As the photopolymerization reactions were very fast, it was difficult to capture the early kinetic reaction with the FTIR imaging system. For 1 wt % initiator, it has been observed that for points A and B the maximum conversion was 83% and 51%, respectively. However, for the system with 5 wt % initiator, the maximum conversion at point A and B were 88% and 73%, respectively. A maximum conversion of 98% and 91% was observed at point A and B, respectively, for the system with 10 wt % initiator.

From Figure 5b, it has been clearly observed that a maximum conversion can be achieved by using high initiator concentration. The higher concentration of initiator generates a large amount of free radicals by absorbing UV light, which consumes the oxygen present in the systems retarding the oxygen inhibition during polymerization. As the initiator concentration increases, the initiation rate and hence the polymerization rates also increase. It also reduces the inhibition period and increases the overall conversion. The effect of oxygen had a great influence on the reaction kinetics of the patterned hydrogel. With an increase in the initiator concentration, the polymerization rate increases correspondingly. The patterned hydrogel produced using these methods are highly uniform in size and shape. Profilometer measurements of hydrogels I, II, and II show average thickness of 2.73, 2.56, and 2.3 μm, respectively. However, the thickness of the patterned hydrogel films depends on the properties of the monomer solution and the applied pressure by the CaF_2 window. Figure 6 shows the optical and SEM images of the patterned hydrogel microstructures.

The effect of different UV intensity on oxygen inhibition during the photopolymerization was also analyzed. For these systems, the same monomer to cross-linker ratio (80:20 mol %) was used. In all cases, 5 wt % DMPA (with respect to total monomer system) was used for the photoinitiator. UV intensities of 6.5, 17.5, and 35.3 mW/cm^2 were applied during polymerization. After application of monomer solutions to the pattern gold surface and covered with CaF_2 window, the reaction assembly was placed on the FTIR microscope stage. The polymerization reactions proceeded as described above, and the spectra were collected at different time intervals. The FTIR images were also extracted from the same peak region and fixed pixel. Figure 7 shows the FTIR images of patterned hydrogels extracted from the 1634 cm^{-1} peak region, with different intensities at different time intervals. From these images, it was clearly observed that hydrogel IV (with intensity 6.5 mW/cm^2) has more unreacted monomer at point B (near the monomer/air interface), while hydrogel VI (with intensity 35.3 mW/cm^2) has less unreacted monomer at the end of the reaction time. A high conversion was also observed in hydrogel VI (Figure 8). However, almost similar conversion was observed in hydrogel V and hydrogel VI at point B. The higher rate of reaction was also observed in hydrogel VI at point A. In order to understand the oxygen inhibition across the thin hydrogel film, we also calculated the conversion with position (i.e., pixel location) from the interface to the center. The distance from the interface toward the center was calculated as the average distance between the two adjacent pixels. The distance of the first pixel from the interface was taken as 2.5 μm. Figures 9 and 10 show the conversions of different hydrogel films across the surface. From Figure 9, it has been clearly observed that for a particular initiator concentration the conversion of monomer gradually increased from the interface toward the center. For a particular pixel, higher conversion was observed for the hydrogel III in comparison to hydrogels I and II. Similar results were also obtained for hydrogels IV, V, and VI. The conversion of the monomer increases from the interface toward the center due to a less significant effect of oxygen.

Conclusion

In summary, a novel method was developed to fabricate hydrogel microstructures on gold surface. The effect of oxygen inhibition during the photopolymerization in a patterned hydrogel thin films was successfully demonstrated by FTIR imaging techniques. Oxygen inhibition was reduced by using higher initiator concentration and high UV intensity. These patterned hydrogel thin films can be used for potential biomedical application, and the unique technique is applicable to a wide variety of hydrogel and other polymeric systems.

References and Notes

(1) Peppas, N. A.; Hilt, J. Z.; Khademhosseini, A.; Langer, R. *Adv. Mater.* **2006**, *18*, 1345.
(2) Pishko, G. L.; Lee, S.-J.; Wanakule, P.; Sarntinoranont, M. *J. Appl. Polym. Sci.* **2007**, *104*, 3730.
(3) Wathier, M.; Johnson, C. S.; Kim, T.; Grinstaff, M. W. *Bioconjugate Chem.* **2006**, *17*, 873.
(4) Ramanan, R. M. K.; Chellamuthu, P.; Tang, L.; Nguyen, K. T. *Biotechnol. Prog.* **2006**, *22*, 118.
(5) Beebe, D. J.; Moore, J. S.; Bauer, J. M.; Yu, Q.; Liu, R. H.; Devadoss, C.; Jo, B. *Nature (London)* **2000**, *404*, 588.
(6) Bhatia, S. N.; Liu, V. A. *Biomed. Microdevices* **2002**, *4*, 257.
(7) Yadavalli, V. K.; Koh, W.-G.; Lazur, G. J.; Pishko, M. V. *Sens. Actuators, B* **2004**, *97*, 290.
(8) Trinh, Q. T.; Gerlach, G.; Sorber, J.; Arndt, K.-F. *Sens. Actuators, B* **2006**, *117*, 17.
(9) Luo, N.; Metters, A. T.; Hutchison, J. B.; Bowman, C. N.; Anseth, K. S. *Macromolecules* **2003**, *36*, 6739.
(10) Basir, R.; Hilt, J. Z.; Gupta, A.; Elibol, O.; Peppas, N. A. *Appl. Phys. Lett.* **2002**, *81*, 3091.
(11) Hilt, J. Z.; Gupta, A. K.; Basir, R.; Peppas, N. A. *Biomed. Microdevices* **2003**, *5*, 177.
(12) Baldi, A.; Lei, M.; Gu, Y.; Siegel, R. A.; Ziaie, B. *Sens. Actuators, B* **2006**, *114*, 9.
(13) Low, L.-M.; Seetharaman, S.; He, K.-Q.; Madou, M. J. *Sens. Actuators, B* **2000**, *67*, 149.
(14) Sershen, S.; Mensing, G.; Beebe, D.; West, J. *Adv. Mater.* **2005**, *17*, 1366.
(15) Chan, K. L. A.; Kazarian, S. G. *J. Comb. Chem.* **2005**, *7*, 185.
(16) Lewis, E. N.; Treado, P. J.; Reeder, R. C.; Story, G. M.; Dowrey, A. E.; Marcott, C.; Levin, I. W. *Anal. Chem.* **1995**, *67*, 3377.
(17) Bhargava, R.; Wang, S.; Keonig, J. L. *Adv. Polym. Sci.* **2003**, *163*, 137.
(18) Fernandez, D. C.; Bhargava, R.; Hewitt, S. M.; Levin, I. W. *Nat. Biotechnol.* **2005**, *23*, 469.
(19) Boskey, A.; Camacho, N. P. *Biomaterials* **2007**, *28*, 2465.
(20) Coutts-Lendon, C. A.; Wright, N. A.; Mieso, E. V.; Keonig, J. L. *J. Controlled Release* **2003**, *93*, 223.
(21) Weerd, Jvan der.; Kazarian, S. G. *J. Controlled Release* **2004**, *98*, 295.
(22) Kazarian, S. G.; AndrewChan, K. L. *Macromolecules* **2003**, *36*, 9866.
(23) Fleming, O. S.; Andrew Chan, K. L.; Kazarian, S. G. *Polymer* **2006**, *47*, 4649.
(24) González-Benito, J.; Koenig, J. L. *Polymer* **2006**, *47*, 3065.
(25) Kazarian, S. G. *Anal. Bioanal. Chem.* **2007**, *388*, 529.
(26) Millan, M. D.; Locklin, J.; Fulghum, T.; Baba, A.; Advincula, R. C. *Polymer* **2005**, *46*, 5556.
(27) Decker, C. *Makromol. Chem.* **1979**, *180*, 2027.
(28) Hoyle, C. E.; Lee, T. Y.; Roper, T. *J. Polym. Sci., Part A: Polym. Chem.* **2004**, *42*, 5301.
(29) Cramer, N. B.; Scott, J. P.; Bowman, C. N. *Macromolecules* **2002**, *35*, 5361.
(30) Dickey, M. D.; Burns, R. L.; Kim, E. K.; Johnson, S. C.; Stacey, N. A.; Wilson, C. G. *AIChE J.* **2005**, *51*, 2547.

(31) O'Brien, A. K.; Bowman, C. N. *Macromol. Theory Simul.* **2006**, *15*, 176.
(32) Kumar, A.; Whitesides, G. M. *Appl. Phys. Lett.* **1993**, *63*, 2002.
(33) Xia, Y.; Whitesides, G. M. *Angew. Chem., Int. Ed. Engl.* **1998**, *37*, 550.
(34) Xia, Y.; Kim, E.; Mrksich, M.; Whitesides, G. M. *Chem. Mater.* **1996**, *8*, 601.
(35) Yan, L.; Zhao, X.-M.; Whitesides, G. M. *J. Am. Chem. Soc.* **1998**, *120*, 6179.
(36) Bernard, A.; Delamarche, E.; Schmid, H.; Michel, B.; Bosshard, H. R.; Biebuyck, H. *Langmuir* **1998**, *14*, 2225.
(37) Biswal, D.; Chirra, H. D.; Hilt, J. Z. *Biomed. Microdevices* **2008**, *10*, 213.
(38) Biswal, D.; Hilt, J. Z. *Polymer* **2006**, *47*, 7355.

MA801600C